Supporting Information

Section 1. Dissipative Particle Dynamics (DPD) method

DPD is a bead-based simulation technique where the motion of beads is governed by the Newton's law of motion. The pairwise force between the beads is made up of three individual forces, namely the conservative force ($\mathbf{F^C}$), the dissipative force ($\mathbf{F^D}$) and the random force ($\mathbf{F^R}$). Those forces can be characterized as

$$\mathbf{F}_{ij}^{C} = a_{ij}\omega^{C}(r_{ij})\mathbf{e}_{ij}$$

$$\mathbf{F}_{ij}^{D} = -\gamma\omega^{D^2}(r_{ij})(\mathbf{e}_{ij}\cdot\mathbf{v}_{ij})\mathbf{e}_{ij}$$

$$\mathbf{F}_{ij}^{R} = \sigma\omega^{R}(r_{ij})\zeta_{ij}\Delta t^{-1/2}\mathbf{e}_{ij}$$

The conservative force acts as the soft repulsion and also identifies the beads with the conservative parameter a_{ij} which differs for different particle species. Without loss of generality, a_{ii}, which acts between the same liquid beads, is set as 25, and a_{sf} between the solid and fluid beads is varied to denote different wettability of the wall. The dissipative force and the random force are coupled together to ensure a canonical equilibrium distribution, serving as a thermostat for the system[1]. All of the three forces are characterized by weigh functions and will vanish in a distance larger than the cut-off radius r_c. All the parameters in a DPD system are scaled by the assemble of the cut-off radius r_c, bead mass m and thermodynamic energy k_BT. For instance, the length, force and time are scaled by r_c, k_BT/r_c and $(mr_c^2/k_BT)^{1/2}$, respectively.

Section 2. The simulation system

As shown in **Figure S1a**, the tube is connected with two reservoirs, which can provide a stable pressure for it. At the beginning of the simulation, no driving force is applied, and the fluid particles diffuse freely for 1×10^4 time steps. The equilibrated distribution of the particles is saved and the actual density in each tube is determined. Then, we remove the reservoirs and take the tube and the fluids inside as the initial conditions for the following simulation (see **Figure S1b**). A body force f_x in the direction of the x-axis is applied on each fluid particle to simulate the pressure gradient. The trajectories of 1×10^6 time steps are used for data analysis.
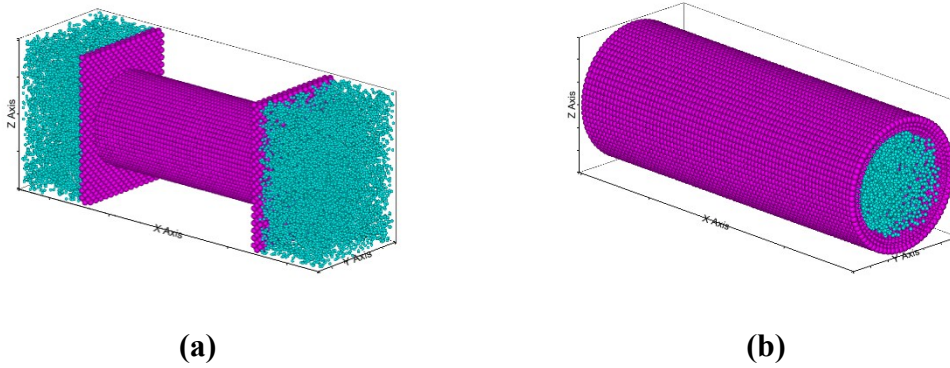

| (a) | (b) |

Figure S1. Scheme of the simulation system: (a) The initial system with reservoirs; (b) The subsequent system without reservoirs.

The repulsive parameter between the solid walls and fluid, a_{sf}, reflects the tube wettability. A brief simulation is conducted to find the relation between a_{sf} and the contact angel of the surface. For the DPD method is not applicable for the systems with different densities, we use another liquid phase to mimic the ambient air as proposed by Kong et al^2. In such method, the conservative parameter between the two

fluids are supposed to be strong (50 in this work) to avoid mixing and the conservative parameter between the ambient phase and the solid is set as 25. In this way, the liquid ambient phase can mimic an air phase in this work. With the results shown in **Figure S2** we choose the values of 25 and 35 to denote the hydrophilic and hydrophobic tubes.
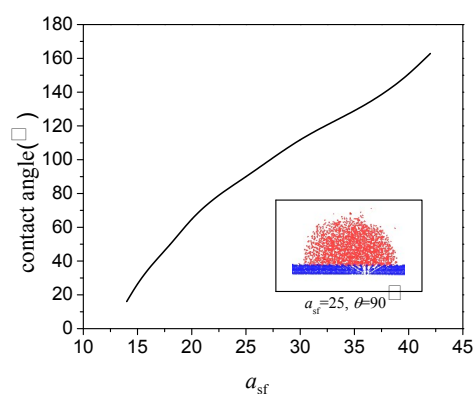

Figure S2. Variation of the contact angle with the repulsive parameter (a_{sf}) obtained from DPD simulation. The inserted figure shows the screenshot of the simulation with a_{sf}=25 and a contact angle of about 90°

Section 3. Appendix to the simulation

The linear relation between the flow rate and the driving force has been shown by tests in two individual tubes, namely the tubes with R=3, a_{sf}=25 and R=3, a_{sf}=35. As shown in Figure S3, the Darcy's law is satisfied with the driving forces we employ in this work.
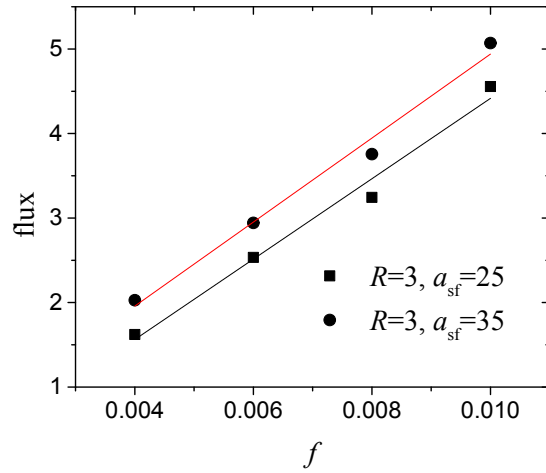
Figure S3. Variation of the flux (beads number/area/time) with the driving acceleration.

In **Figure S4**, the density profiles within the same tube ($R=4$, $a_{sf}=35$) in different flow states are displayed. The profiles, no matter in static or dynamic state with various driving forces, all coincide with each other. Therefore, we draw a conclusion that in the velocity scope involved in this work ($Re<10$), the density profile exclusively depends on the tube, and is independent on the flow state.
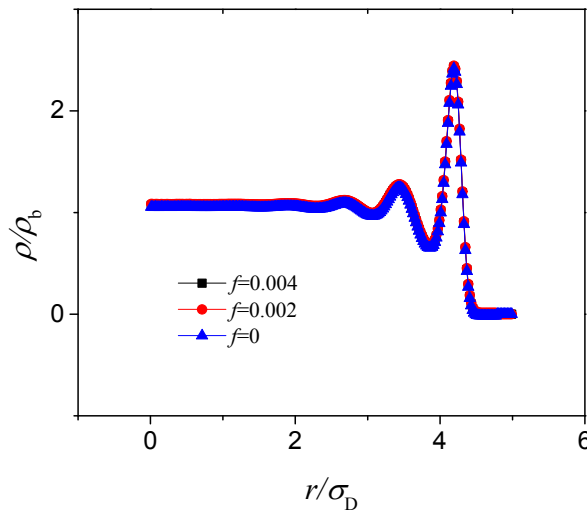

Figure S4. Density profiles within the tube of $R=5$ and $a_{sf}=35$ under different

driving forces.

Figure S5 shows the velocity profiles in nanotubes. The profiles exhibit various characters with different tube sizes. **In Figure S5a**, the radius is $23\sigma_D$ and the inhomogeneous region can be approximately ignored. However, the slip at the solid-liquid interface is obvious. The radius in **Figure S5b** is $8\sigma_D$, and the inhomogeneous region can be clearly seen. The Hagen-Poiseuille velocity profile is also depicted in this figure (the red spots). Both of the profiles start at zero at the walls while their summit velocities are far apart. So we can draw a conclusion that the inhomogeneous boundary evidently enhances the general velocity in nanotubes. When the radius falls to less than $3\sigma_D$ in **Figure S5c**, the plug-flow with a uniform velocity takes place. In this case, the inhomogeneous region overlaps and leads to an ultra-high viscosity in the central area.
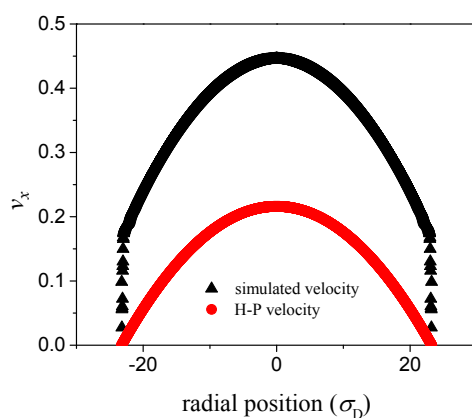

(a)
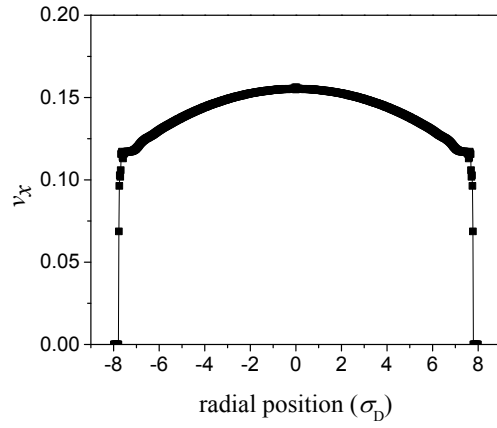
(b)
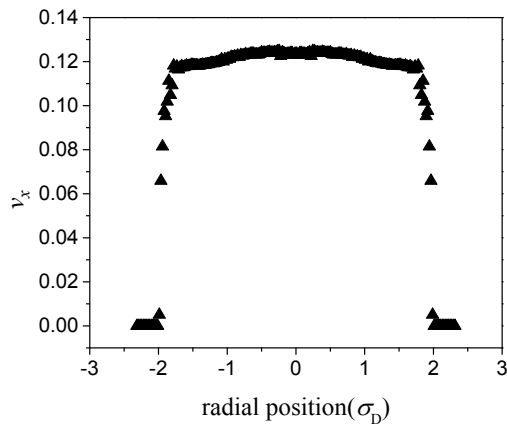
(c)

Figure S5. Velocity profiles in nanotubes with different radiuses.

To certify the DPD results, we make a comparison with the Lennard-Jones fluid in previous works[3] (**Figure S6**), where the nonequilibrium molecular dynamics (NEMD) method is employed. The quantitative differences lie in the structural variance (it is the nano-slit in Ref.2) and interactional difference. It denotes that the DPD method is adequate to show the inhomogeneity of fluid even though some details on electronic level have been ignored.
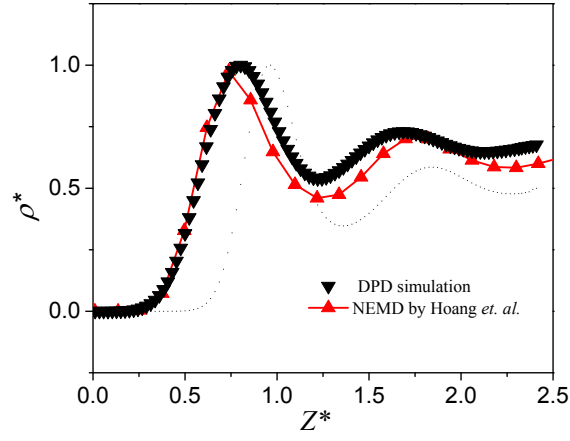
(a)
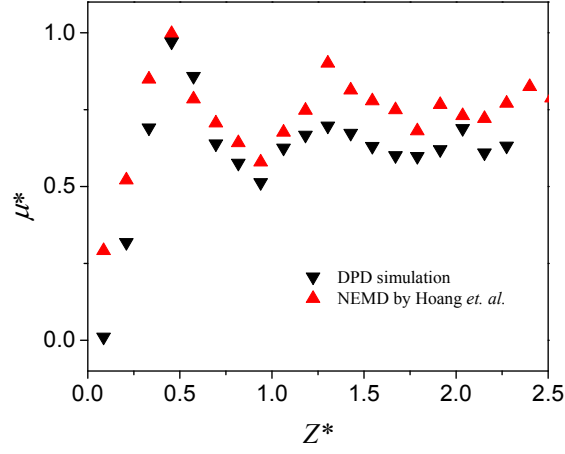
(b)

Figure S6. Comparison of normalized density and viscosity profiles by DPD and NEMD simulation in nanotubes.

Section 4. The details in derivation

From the stokes equation with viscosity and density distribution,

$$\frac{1}{r}\frac{\mathrm{d}}{\mathrm{d}r}\left(r\mu(r)\frac{\mathrm{d}v_x}{\mathrm{d}r}\right) = -\rho(r)f_x$$

Within the inhomogeneous region, it is assumed that the fluid velocity at the fluid-solid boundary equals zero. And the fluid velocity at the inhomogeneous-bulk interface is v_s. One can get the velocity distribution function in the inhomogeneous region as

$$v_x^i(r) = \left[v_s + \int_{R-\delta}^{R} \frac{\int_r^R r'\rho(r')f_x\,\mathrm{d}r'}{r\mu(r)}\,\mathrm{d}r \right]\left[\frac{\int_r^R \frac{\mathrm{d}r}{r\mu(r)}}{\int_{R-\delta}^{R} \frac{\mathrm{d}r}{r\mu(r)}} \right] - \int_r^R \frac{\int_r^R r'\rho(r')f_x\,\mathrm{d}r'}{r\mu(r)}\,\mathrm{d}r$$

where r equals zero at the center and equals R at the solid face. In the bulk region, however, one has $\mu(r) = \mu_b$ and $\rho(r) = \rho_b$. With v_s as the boundary condition, the velocity distribution gives

$$v_x^b(r) = v_s + \frac{\rho_b f_x}{4\mu_b}\left[(R-\delta)^2 - r^2 \right]$$

v_s can be determined by the matching of the inhomogeneous and the bulk regions as

$$v_s = \left[\frac{\rho_b f_x (R-\delta)\delta}{2} + \int_{R-\delta}^{R} r\rho(r)f_x\,\mathrm{d}r \right] \cdot \int_{R-\delta}^{R} \frac{\mathrm{d}r}{r\mu(r)} - \int_{R-\delta}^{R} \frac{\int_r^R r'\rho(r')f_x\,\mathrm{d}r'}{r\mu(r)}\,\mathrm{d}r$$

By integrating the velocity expressions on the cross section, one can get the penetration rate as

$$\frac{Q}{f_x} = \frac{1}{\pi R^2}\left[\int_{R-\delta}^{R} \rho(r)v_x^i(r)\cdot 2\pi r\,\mathrm{d}r + \int_0^{R-\delta} \rho v_x^o(r)\cdot 2\pi r\,\mathrm{d}r \right]$$

$$= \frac{\rho_b^2 R^2}{\mu_b}\left[\begin{array}{l} \left(\dfrac{\delta}{R}\right)^4\left(\dfrac{A_1}{2R}+\dfrac{1}{8}\right) + \left(\dfrac{\delta}{R}\right)^3\left(-\dfrac{3A_1}{2R}+\dfrac{1}{2}\right) - \left(\dfrac{\delta}{R}\right)^2\left(-\dfrac{3A_1}{2R}+\dfrac{3}{4}\right) \\ + \left(\dfrac{\delta}{R}\right)\left(\dfrac{A_1}{2R}-\dfrac{A_2}{R^2}-\dfrac{1}{2}\right) + \left(\dfrac{A_2}{R^2}+\dfrac{2A_3}{R^3}+\dfrac{1}{8}\right) \end{array} \right]$$

where

$$A_1 = \int_{R-\delta}^{R} \frac{R\mu_b}{r\mu(r)} \, dr$$

$$A_2 = \int_{R-\delta}^{R} \frac{R\mu_b \int_{R-\delta}^{r} \frac{r'\rho(r')}{R\rho_b} \, dr'}{r\mu(r)} \, dr$$

$$A_3 = \int_{R-\delta}^{R} \frac{r\rho(r)}{R\rho_b} \left[\int_{r}^{R} \frac{R\mu_b \int_{R-\delta}^{r'} \frac{r''\rho(r'')}{\rho_b} \, dr''}{r'\mu(r')} \, dr' \right] dr$$

As the apparent slip emerges as the extrapolation of the bulk velocity profile at the boundary, it is defined as

$$v_x^b(R) - v_{wall} = -\lambda \left. \frac{dv_x^b}{dr} \right|_{r=R}$$

according to the Navier's boundary condition. Then the expression of the slip length can be given as

$$\lambda = \frac{(R-\delta)\delta}{R_2} \int_{R-\delta}^{R} \frac{R\mu_b}{r\mu(r)} \, dr + \frac{2}{R} \left(\int_{R-\delta}^{R} \frac{R\mu_b \int_{R-\delta}^{r} \frac{r\rho(r)}{R\rho_b} \, dr}{r\mu(r)} \right) + \frac{\delta^2}{2R} - \delta$$

It is revealed that the slip length is related to both the density and viscosity distributions in the inhomogeneous region. Accordingly, the expression can be simplified as

$$\lambda = A_1 \frac{(R-\delta)\delta}{R^2} + \frac{2}{R} A_2 + \frac{\delta^2}{2R} - \delta$$

The effective slip is calculated from the Navier's equation

$$\frac{Q}{f_x} = \frac{\rho_b^2 R^2}{8\mu_b}\left[1 + \frac{\lambda}{4R}\right]$$

Thus the effective slip length can be given as

$$\lambda = 4R(\varepsilon - 1)$$

where ε is the flow enhancement. The effective slip length is the surface slip length in need to produce the particular enhancement when the velocity profile is assumed to be a smooth parabola. The apparent slip, on the other hand, is based on the actual velocity profiles. When the inhomogeneity cannot be ignored and the velocity profile is severely distorted, there can be evident differences between those two kinds of slippage. And as the tube radius gets larger, the two slip lengths get close to each other.

Section 5. Converting DPD units to real scale

When the DPD beads serve as simple liquid model that can be considered as individual water molecules with a number density of 3, the effective diameter of one molecule is $0.86r_C$, which can be obtained by the radial distribution function. In real life the effective diameter of water molecules in normal state is 0.4 nm. Hence, we have

$$r_C \approx 5 \times 10^{-10}\,[\text{m}]$$

According to Stokes-Einstein equation, the diffusion constant of water molecules is

$$D = \frac{k_B T}{3\pi\eta\sigma_b} \approx \frac{5\times10^{-19}}{r_C}[\mathrm{m}]$$

which works out at $D\approx1\times10^{-9}\mathrm{m}^2$ s^{-1}. In DPD simulation, the statistical result of the diffusion constant by Green-Kubo theory is $D_{\mathrm{DPD}}\approx0.3$ r_C^2 τ^{-1}. Equating the diffusion constants in the simulation and in the physical system, we get

$$\tau \approx 6\times10^{-11}[\mathrm{s}]$$

Therefore the velocity scale is

$$r_C/\tau \approx 10[\mathrm{m}\cdot\mathrm{s}^{-1}]$$

Thus the order of magnitude of the velocity results in this work is about 1×10^{-1} m/s.

[1] Español, P.; Warren, P. Statistical mechanics of dissipative particle dynamics. *Europhys. Lett*. 1995, 30, 191-196.

[2]. Kong, B.; Yang, X. Dissipative Particle Dynamics Simulation of Contact Angle Hysteresis on a Patterned Solid/Air Composite Surface. *Langmiur,* 2006, 22, 2065-2073.

[3] Hoang, H.; Galliero, G. Local viscosity of a fluid confined in a narrow pore, *Phys. Rev. E,* 2012, 86, 021202.

[4] Babu, J. S.; Sathian, S. P. The role of activation energy and reduced viscosity on the enhancement of water flow through carbon nanotubes. *J. Chem. Phys*. 2011, 134, 194509.